

## Low-temperature properties of crystalline $(\text{KBr})_{1-x}(\text{KCN})_x$ : A model glass

J. J. De Yoreo\*

*Laboratory of Atomic and Solid State Physics, Cornell University, Ithaca, New York 14853-2501*

W. Knaak†

*Institut für Festkörperphysik, Technische Universität Berlin, D-1000 Berlin 12, Federal Republic of Germany*

M. Meissner

*Laboratory of Atomic and Solid State Physics, Cornell University, Ithaca, New York 14853-2501,  
Institut für Festkörperphysik, Technische Universität Berlin, D-1000 Berlin 12, Federal Republic of Germany,  
and Hahn-Meitner Institut für Kernforschung, D-1000 Berlin 39, Federal Republic of Germany*

R. O. Pohl

*Laboratory of Atomic and Solid State Physics, Cornell University, Ithaca, New York 14853-2501*

(Received 30 June 1986)

The thermal properties of  $(\text{KBr})_{1-x}(\text{KCN})_x$  single crystals have been studied between 0.05 and 100 K over the entire compositional range. For  $0.25 \leq x \leq 0.70$ , these crystals have the thermal conductivity that is typical for all structurally disordered, amorphous solids. The same holds for the low-temperature specific heat, which varies linearly with temperature, and logarithmically with the measuring time. Through a quantitative analysis it is shown that these mixed crystals represent an excellent example of two-level-system excitations of variable number densities, depending on the choice of  $x$ . Therefore, these crystals can serve as a model for the exploration of the low-energy excitations which are characteristic for all amorphous solids.

### I. INTRODUCTION

The vibrational properties of structurally amorphous solids differ from those of crystalline solids in many ways, and are still only poorly understood. One approach to their study is to search for similar properties in crystalline solids in which the disorder is carefully controlled and, hopefully, easier to understand.<sup>1</sup> The present investigation deals with single crystals of  $(\text{KBr})_{1-x}(\text{KCN})_x$ . For low cyanide concentrations,  $x \leq 0.001$ , the cyanide ions can perform a quasirotational tunneling motion even at the lowest temperatures.<sup>2,3</sup> Their equilibrium orientations lie along the eight  $\langle 111 \rangle$  directions in the bromine vacancies the  $\text{CN}^-$  ions occupy.<sup>4,5</sup> As the molar fraction  $x$  of the dissolved KCN increases beyond 0.001, interactions between the cyanide ions become important, and the low-temperature thermal,<sup>5-8</sup> dielectric,<sup>7</sup> and ultrasonic<sup>9</sup> properties become increasingly more like those of structurally amorphous solids.

In this paper, we present a detailed study of the thermal conductivity and the specific heat including its time dependence, of this mixed crystal system between 0.05 and 100 K, over the entire compositional range. Glasslike properties are observed for mixed crystals with  $x=0.25$ , 0.50, and 0.70. Some of the results have been reported previously.<sup>6,8</sup>

The paper is organized as follows: In Sec. II we describe the experimental techniques for sample preparation and for the measurements of the thermal conductivity, thermal diffusivity, and specific heat including its time dependence. In Sec. III, the elastic constants required for

the analysis have been summarized, largely from the literature. The experimental results are presented in Sec. IV. In Sec. V we show that the data can be well described using, in the framework of the standard tunneling model, tunneling states interacting with Debye phonons. We discuss the limitations of the picture<sup>8,10</sup> that the tunneling centers are caused by a very small fraction of  $\text{CN}^-$  ions which happen to retain their quasirotational mobility. Finally, we present evidence that the onset of interactions between  $\text{CN}^-$  ions for  $x > 10^{-3}$  is via electric dipoles, and briefly discuss the thermal conductivity above 1 K.

### II. EXPERIMENTAL MATTERS

#### A. Safety

Because of their toxicity, work with cyanides requires certain precautions.<sup>11</sup> Cyanides can enter the body by inhalation of powder or by absorption through the skin. However, if handled with plastic gloves and if no powder is inhaled, they present no danger. As a safety precaution, grinding of crystals should be done in a glove box or a disposable glove bag. The presence of an acidic solution, however, will lead to the production of hydrogen cyanide via the reaction  $\text{MCN} + \text{HCl} \rightarrow \text{MCl} + \text{HCN}$ , and this latter gas is extremely toxic. Thus, the most important precaution required in handling cyanides is to avoid exposing them to acidic solutions such as soldering flux.

Alkali cyanides are somewhat hygroscopic. Thus, exposure to air for extended periods of time leads to deterioration of the sample. The use of a heat lamp will

help in that case.

The safety precautions mentioned here have been found useful in handling KCN-rich crystals. They should also be adequate for NaCN, while RbCN and in particular CsCN require greater care.<sup>12</sup>

### B. Sample (Ref. 13)

The crystals were seedpulled from the melt under a protective atmosphere, using bromine treated KBr and zone refined KCN, in the Crystal Growing Facility of the Materials Science Center at Cornell University. Several of the samples were supplied by S. Susman from the Argonne National Laboratories and from F. Lüty and M. Delong of the University of Utah's crystal growing facility. The  $\text{CN}^-$  concentration was determined through optical absorption of the stretching vibration (fundamental or overtone), using the conversion factors determined previously by chemical analysis.<sup>3</sup> In the high-concentration region, the optically determined concentrations agreed with those in the melt within the experimental accuracy ( $\pm 3\%$ ). This agreement demonstrates the excellent miscibility of KBr and KCN. (Pieces from the boule with  $x=0.70$  in the melt were also studied by Rowe. From the lattice parameter and from the transition temperature, he determined  $x=0.74$ .<sup>12</sup>) The  $(\text{NaCN})_{0.75}(\text{KCN})_{0.25}$  sample was obtained from F. Lüty.

### C. Thermal conductivity (Ref. 13)

Thermal conductivity was measured with the steady-state temperature gradient method, using standard  $^4\text{He}$  and dilution cryostats to cover the temperature range  $\sim 150$  to  $0.05$  K. As usual, cleaved samples  $5 \times 5 \times 50$  mm were preferred. If only much smaller samples were available, heaters and thermometers were attached to thin copper wires glued to the samples with GE 7031 varnish, which was found not to react with the samples. The surfaces were sandblasted to ensure diffuse phonon scattering.

### D. Thermal diffusivity (Ref. 13)

Thermal diffusivity measurements above 2 K were performed on  $\text{KBr}_{0.90}\text{KCN}_{0.10}$  and  $\text{KBr}_{0.75}\text{KCN}_{0.25}$ . The method, which has been described in detail elsewhere,<sup>14</sup> enabled us to determine both the specific heat and the thermal conductivity. The thermometer consisted of a ground-down Allen Bradley carbon resistor to which copper leads were attached with silver paint (Dupont 4922). The resistor was then dipped in epoxy (Stycast 1266). The thermometer was glued to the sample with varnish (GE 7031). The heater consisted of a constantan film evaporated on one face of the sample. To ensure uniform heating, the film was laid down in a meander across the face. Thin copper leads were epoxied to either end of the meander. The temperature-time profile was recorded with a transient recorder and analyzed with the aid of a computer. Thermal conductivity and diffusivity measurements agreed to within the errors in estimating the geometry.

### E. Long-time specific heat

Long-time specific heat measurements were performed with the transient heat pulse technique used previously at Cornell.<sup>15</sup> Thermal sample-to-bath time constants were typically of the order of 10–100 s. Samples with a mass of the order of 1 g were mounted between sapphire pins which were thermally well anchored to the heat sink. Either an evaporated constantan film or a Pt-W, 1 mil diameter wire glued to the sample were used as heaters, a small chip of a Speer 220- $\Omega$  resistor, encapsulated in glue, was attached as thermometer. The thermal time constant was determined by a properly chosen thin copper wire, one end of which was soldered to a small piece of copper foil, which in turn was glued to the sample. The heat capacity of the addenda was estimated and was corrected for if found to be non-negligible. The exponential decay of the temperature rise was recorded and used to evaluate the heat capacity with the aid of a computer.

### F. Time-dependent specific heat (Ref. 16)

The experimental arrangement (Fig. 1) was similar to that for transient heat pulse measurements. Sample-to-bath time constants  $\tau_{RC}$  varied between 0.5 and 10 s. As thermal links three thin ( $\sim 1$  mm diameter) copper rods were used, to which the sample was attached with minute amounts of GE-7031 varnish. By utilizing both a short-time thermometry technique ( $\tau_{th} \approx 1$  to  $10 \mu\text{s}$ ) and fast phonon thermalization ( $\tau_D \approx 10$  to  $100 \mu\text{s}$ ), i.e., a very thin

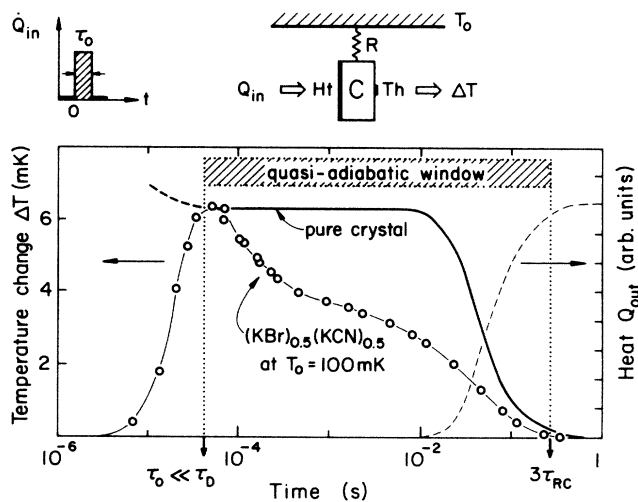


FIG. 1. Top: Schematic setup for measurements of time-dependent specific heat. Bottom: Two traces of  $\Delta T(t)$  are shown: For the pure crystal, the trace is only schematic, and omits, for example, the ballistic signals (Ref. 17); for  $(\text{KBr})_{0.5}(\text{KCN})_{0.5}$ , the data points represent actual measurements. After the thermalization time  $\tau_D$ ,  $\Delta T$  for the pure crystal remains constant until the sample-to-bath relaxation time  $\tau_{RC}$  has been reached. In  $(\text{KBr})_{0.5}(\text{KCN})_{0.5}$ ,  $\Delta T(t)$  is a direct measure of the thermalization of the weakly coupled defect states. The hump seen in the experimental trace at  $\sim 10^{-2}$  s marks the beginning of the heat draining from the sample. This effect, however, can be corrected for, and thus the quasiadiabatic time window extends to  $\approx 3\tau_{RC}$ , as indicated.

TABLE I. Compilation of low-temperature data on the elastic properties, specific heat, and thermal conductivity of single crystals of  $(\text{KBr})_{1-x}(\text{KCN})_x$ . The following quantities are listed (in their dependence on  $x$ ): The second column gives the molecular weight  $M$ , i.e., the mass of a sample containing  $6.02 \times 10^{23}$  (1 mol) potassium ions, calculated by linear interpolation between KBr and KCN. The third column gives the mass density  $\rho$  at low temperatures, Ref. 13. The fourth through sixth columns give the elastic constants  $c_k$  at 4 K, compiled from various sources, as summarized in Ref. 18. The values of  $c_{11}$  and  $c_{44}$  are believed to be accurate to  $\pm 5\%$ , those for  $c_{12}$  to  $\pm 15\%$ . The seventh column gives the Debye velocity  $v_D$ , calculated from the harmonic series expansion method (Ref. 19), using the values given in the third through sixth columns (see, however, also footnote a). The eighth column gives the Debye temperature  $\Theta_D$ : Note that for this calculation, the number density of atoms is needed; we have counted the  $\text{CN}^-$  ion as one atom, i.e., ignored its rotational and internal degrees of freedom. The ninth column gives the calculated prefactor  $C(T \rightarrow 0 \text{ K}) = c_D T^3$ , using the values given in the third through seventh columns. The tenth and eleventh columns give the prefactors  $c_1$  and  $c_3$  from the fit of the long-time ( $\sim 10$  s) specific-heat data to  $C(T) = c_1 T + (c_D + c_3) T^3$  [Eq. (2)], see also Fig. 10. The twelfth column gives the spectral density  $\bar{P}(x)$  of tunneling centers, from fit of time-dependent specific-heat data as shown in Fig. 11, with the aid of Eq. (8). The thirteenth column gives the prefactor  $A$ , from fit of thermal-conductivity data to  $\Lambda = AT^2$ ; note, however, that this is not necessarily the best fit to the data, see text and Fig. 13. The last column gives the averaged coupling constant  $\bar{\gamma}$ , calculated from Eq. (12) using the values given in the third, seventh, twelfth, and thirteenth columns. Note that some of the values given in this table differ somewhat from those given earlier (Refs. 8 and 13). The present values are based on more recent measurements of  $C_p(T, t)$  for  $x=0.25$  and on a completely new evaluation of all our data.

$x$	$M$ (g/mol)	$\rho$ (g/cm <sup>3</sup> )	$c_{11}$ ( $10^{10}$ N/m <sup>2</sup> )	$c_{12}$ ( $10^{10}$ N/m <sup>2</sup> )	$c_{44}$	$v_D$ ( $10^3$ m/s)	$\Theta_D$ (K)	$c_D$ ( $10^{-7}$ J/gK <sup>4</sup> )	$c_3$ ( $10^{-7}$ J/gK <sup>4</sup> )	$c_1$ ( $10^{-7}$ J/gK <sup>2</sup> )	$\bar{P}$ ( $10^{14}$ /J m <sup>3</sup> )	$A$ ( $10^{-4}$ W/cm K <sup>3</sup> )	$\bar{\gamma}$ (eV)
0	119.00	2.82	4.17	0.52	0.520	1.88	171	65.2	70 $\pm$ 7 <sup>d</sup>				
0.05	116.30	2.76	3.40	0.75	0.380	1.63	148	102					
0.10	113.60	2.69	3.20	0.85	0.350	1.58	144	115					
0.25	105.50	2.50	3.01	1.00	0.306	1.54	140	134	76	24	40 $\pm$ 4	9.5	0.12
0.50	92.06	2.18	2.84	1.10	0.240	1.48	135	173	11	9.0	9 $\pm$ 1	17	0.18
0.70	81.28	1.95				1.63 <sup>a</sup>	148 <sup>a</sup>	146 <sup>b</sup>	84	4.3	2.7 $\pm$ 0.3	7.5	0.48
1.0	65.11	1.60	2.70		0.325	1.95 <sup>a</sup>	180 <sup>a</sup>	103 <sup>c</sup>	103 $\pm$ 8 <sup>d</sup>				

<sup>a</sup>Calculated from  $c_D$ .

<sup>b</sup>Linear interpolation between  $x=0.5$  and  $x=1$ .

<sup>c</sup>From assumption  $c_D = c_3$ .

<sup>d</sup>Not excess contribution; obtained from average of  $C_p/T^3$  data (see Fig. 7).

sample, we were able to observe the time dependence in a quasiadiabatic time window of  $10^{-5} \text{ s} < t_{\text{exp}} < 10 \text{ s}$  in which internal relaxation processes can be interpreted as a time-dependent specific heat.

In order to reduce addenda heat capacities we used an evaporated gold film heater ( $\approx 20 \text{ nm}$  thick) and rubbed-on carbon film thermometer ( $\approx 500 \text{ nm}$  thick) leading to a total addendum capacity  $\approx 10^{-8} T \text{ (J/K}^2\text{)}$ . A short heat pulse ( $\tau_0 \approx 1 \mu\text{s}$ ) was uniformly applied on one side of the sample which was shaped like a thin plate. The temperature profile  $\Delta T(t)$  at the other side of the sample was monitored by the small (area  $\approx 1 \text{ mm}^2$ ) carbon film thermometer. For an ideal crystalline Debye solid, thermalization takes place by inelastic diffusive phonon scattering at the surface, leading to an equilibrium temperature  $T = T_0 + \Delta T$  within  $< 50 \mu\text{s}$  (for  $T > 0.1 \text{ K}$ ).<sup>17</sup> The temperature rise  $\Delta T(t)$  remains constant over decades of time (see solid curve in Fig. 1) until the heat drains out of the sample through the thermal link. This heat flux out of the sample at times  $t_{\text{exp}} \approx \tau_{RC}$  can be corrected for up until the signal-to-noise ratio becomes unacceptably large. Thus, the time-dependent specific heat is calculated by

$$C_p(t) = \frac{Q_{\text{in}} - R^{-1} \int_0^t \Delta T(t') dt'}{m \Delta T(t)}, \quad (1)$$

where  $R$  is the thermal resistance of the thermal link and  $m$  is the sample mass.

For solids in which, in addition to the phonon system, other excitations are present, which can couple to the phonon bath within the adiabatic time window, the decrease of  $\Delta T(t)$  due to the relaxation process can be detected for times up to  $3\tau_{RC}$ . As an example, we see in Fig. 1 a trace of  $\Delta T$  versus  $\log t$  which was measured for  $(\text{KBr})_{0.5}(\text{KCN})_{0.5}$  at  $T_0 = 0.1 \text{ K}$ . As the heat diffuses through the sample of thickness  $d \approx 0.5 \text{ mm}$ , the temperature rise  $\Delta T(t)$  reaches a maximum at  $\tau_D \sim d^2/D$  ( $D$  is the thermal diffusivity; at  $0.1 \text{ K}$ ,  $D \approx 50 \text{ cm}^2/\text{s}$ ). It is followed by a slow decay.

The temperature profiles for at least four different ranges of time were collected with the help of a signal averager, using 100 to 1000 pulses. The time-dependent specific-heat profiles were analyzed with the help of a microcomputer. This technique was developed in Berlin, and has also been used by one of us (M.M.) at Cornell.

### III. ELASTIC DATA AND DEBYE APPROXIMATION

In order to evaluate thermal conductivity and specific heat, the Debye sound velocity and specific heat were needed. The three elastic constants  $c_{11}$ ,  $c_{12}$ , and  $c_{44}$  at  $4 \text{ K}$  are listed in Table I,<sup>18</sup> together with the molecular weights and the mass densities  $\rho(x)$ . The Debye velocities  $v_D$ , temperatures  $\Theta_D$ , and specific heats  $C_D = c_D T^3$  were calculated from these quantities,<sup>19</sup> and are also listed in Table I. For details, see the caption. Figure 2 shows the dependence of  $c_D$  and  $\Theta_D$  on  $x$ . Note the problems involved in determining  $c_{ik}$  and  $\Theta_D$  for  $x > 0.56$ , since the  $(\text{KBr})_{1-x}(\text{KCN})_x$  lattice undergoes various phase transitions from cubic to orthorhombic to monoclinic symmetry at low temperatures (see Table I).<sup>20</sup> Nevertheless,

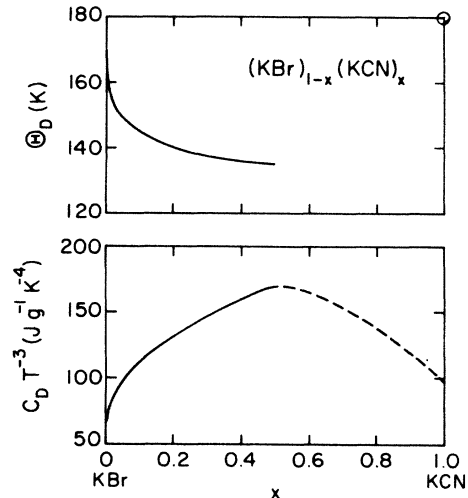


FIG. 2.  $C_D$ , the Debye specific heat, divided by  $T^3$ , and the Debye temperature,  $\Theta_D$ , the latter derived from ultrasonic measurements [except for pure KCN, for which crystal  $C_D$  and  $\Theta_D$  (note the data point) were determined from specific-heat measurements], see Table I. Note that  $\Theta_D$  rises rapidly as  $x$  approaches zero, reaching  $171 \text{ K}$  for  $x=0$ . For  $x > 0.56$ , no  $\Theta_D$  was calculated because of the low-temperature crystallographic phase transitions (Ref. 20). Dashed line: interpolation.

there is clear evidence for a maximum in  $c_D$  in the middle of the composition range.

### IV. EXPERIMENTAL RESULTS

Figure 3 shows an extension of the thermal-conductivity measurements by Seward and Narayanamurti<sup>3</sup> to lower temperatures and also to higher concentrations. The resonance interaction of the thermal phonons with the tunneling states of the isolated  $\text{CN}^-$  ions which leads to the dip in the thermal conductivity around  $0.5 \text{ K}$  is still clearly discernible at the KCN molar fraction  $x=0.003$ . However, as  $x$  is increased beyond this value, the conductivity ceases to decrease further. For  $x=0.01$  (not shown here), a concentration studied by Moy *et al.*,<sup>7</sup> the conductivity curve is, in fact, approximately 50% higher at the lowest temperatures than our curve for  $x=0.003$ , crosses it at  $\sim 1 \text{ K}$ , and is lower only at higher temperatures. This behavior shows the onset of an interaction between the cyanide ions. A further increase of  $x$  to  $0.05$  causes the dip at  $0.5 \text{ K}$  to vanish (see Fig. 3) while above a few degrees K the conductivity still decreases. The same trend persists as  $x$  increases further (Fig. 4). For  $x \geq 0.25$ , however, the thermal conductivity resembles that of amorphous solids qualitatively as well as quantitatively. This is illustrated in Fig. 5 by the two dashed curves, for  $\alpha\text{-As}_2\text{S}_3$  and for  $\alpha\text{-SiO}_2$ ,<sup>21</sup> which essentially span the entire range of thermal conductivity of all amorphous solids measured in the temperature range below  $\approx 10 \text{ K}$ . Glasslike thermal conductivity also persists for  $x=0.70$ , also shown in Fig. 4. For  $x=1.0$ , i.e., pure KCN, however, the thermal conductivity shows the behavior of a crystalline, albeit disordered solid (Fig. 6):

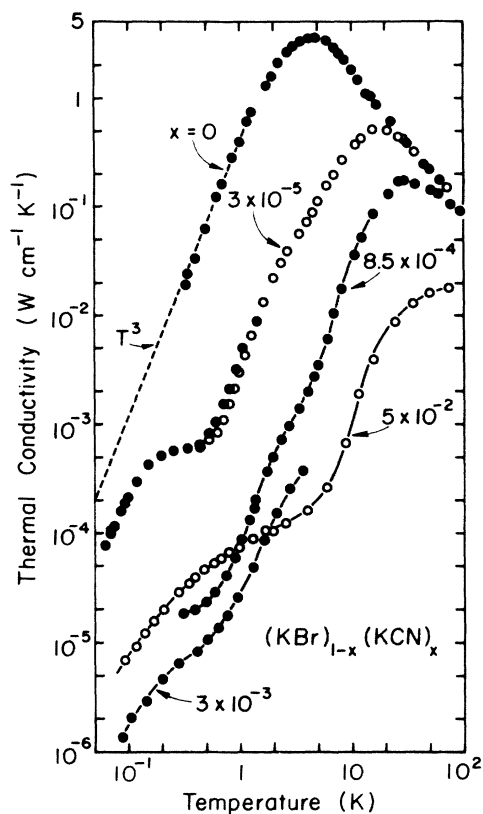


FIG. 3. Thermal conductivity of  $(\text{KBr})_{1-x}(\text{KCN})_x$ :  $x=0$ ,  $3 \times 10^{-5}$  (above 0.3 K) and  $x=8.5 \times 10^{-4}$  after Ref. 3;  $x=3 \times 10^{-5}$  (same sample as that of Ref. 3, for  $T < 2$  K),  $x=3 \times 10^{-3}$ , and  $5 \times 10^{-2}$ , this study. Note that the value of  $x=8.5 \times 10^{-4}$  differs from that given in Ref. 3 ( $5 \times 10^{-4}$ ). The value given here is based on a critical reevaluation of the infrared absorption in this sample.

The thermal conductivity increases with decreasing temperature, goes through a maximum, and then decreases. Below 1 K, the conductivity is very much smaller than that of amorphous solids. The defects giving rise to this low-temperature phonon scattering are believed to be domain walls as will be discussed later. The important observation at this point is that the glasslike thermal conductivity is observed in the range  $x=0.25$  to  $x=0.70$  but not for  $x=1$ .

Tunneling states of isolated impurities can be observed in specific-heat measurements.<sup>3</sup> The presence of 30 part per million (ppm) of  $\text{CN}^-$  substituting for an equal number of  $\text{Br}^-$  ions leads to an increase of the specific heat at 0.1 K by over one order of magnitude over the  $T^3$  specific heat of pure KBr [see Fig. 7(a)]. This Schottky-type anomaly, believed to be slightly broadened in this case because of a distortion of the cubic environment around the  $\text{CN}^-$  ions,<sup>22,23</sup> scales with  $x$  for  $x < 8.5 \times 10^{-4}$ . A further increase in  $x$  [by a factor of 60, Fig. 7(b)] yields for  $x=0.05$  almost the same magnitude of the specific heat as for  $x=8.5 \times 10^{-4}$  (at 0.1 K). As  $x$  increases up to  $x=0.70$ , the specific heat decreases drastically. Schottky anomalies are not observed for  $x \geq 0.05$ . Instead, a linear temperature dependence is approached at the lowest tem-

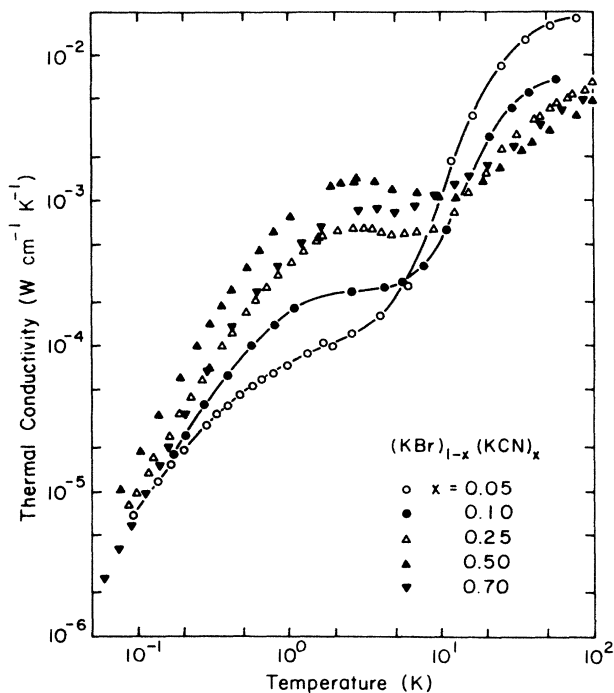


FIG. 4. Thermal conductivity for  $x$  ranging from 0.05 to 0.70. Measurements by Moy *et al.*, Ref. 7, taken below 10 K, agree well with our data. For  $x > 0.25$ , the conductivity is almost independent of  $x$ . Note that the data for  $x=0.70$  drop off somewhat more rapidly at the lowest temperatures. An explanation is offered in the text.

peratures for  $x \geq 0.25$ ; it will be shown below that its magnitude is close to that of structural glasses.

The data shown in Fig. 7(b), and extended to higher temperatures, are replotted as  $C_p/C_D$  versus  $T$  in Fig. 8, where  $C_p$  is the measured specific heat and  $C_D$  is the calculated Debye specific heat ( $\Theta_D$  from Table I). KBr (Refs. 24 and 25) and KCN show a behavior typical for reasonably pure crystals: below 5 K (i.e.,  $\approx 3\%$  of  $\Theta_D$ , generally speaking)  $C_p$  agrees well with the Debye prediction. Around 15 K ( $\approx 0.1\Theta_D$ ),  $C_p/C_D$  goes through a maximum for both KBr and KCN. This, too, is common, and is explained with a peak in the transverse acoustic phonon density of states for frequencies having wave vectors near the zone boundary.<sup>26</sup> For the range of composition for which the thermal conductivity shows glasslike behavior this peak is also visible, but it is shifted to lower temperatures (2 to 5 K; the data for  $x=0.53$  are due to Mertz and Loidl, Ref. 27). This shift is also characteristic for structural glasses.<sup>28</sup>

A logarithmic time dependence is another characteristic feature of the specific heat of structural glasses.<sup>29-31</sup> A time dependence has also been found in  $(\text{KBr})_{x-1}(\text{KCN})_x$ , see Fig. 9. It will be shown below that in the compositional range in which thermal conductivity and (long-time) specific heat show a glasslike behavior ( $x=0.25, 0.50$ , and  $0.70$ ), the specific heat varies as the logarithm of the measuring time. The upper limit of the temperature at which a time dependence of the specific heat is no longer observable (within the quasiadiabatic

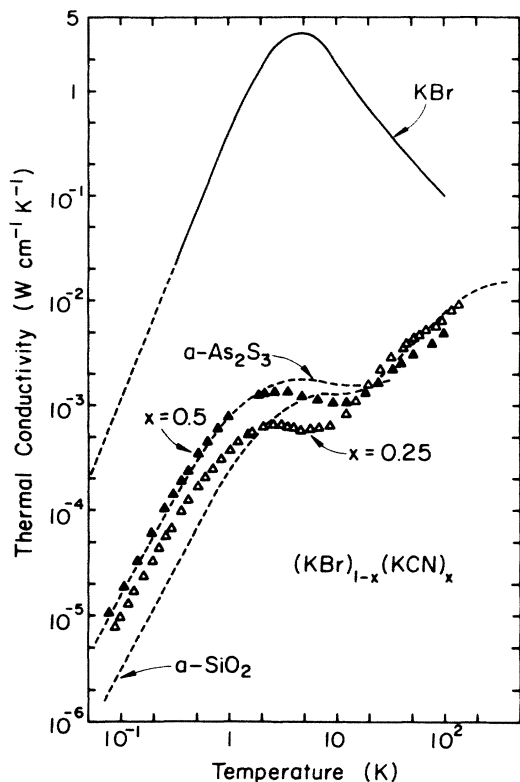


FIG. 5. Thermal conductivity for  $x=0.25$  and  $0.50$ . The two dashed curves for  $\alpha\text{-As}_2\text{S}_3$  and  $\alpha\text{-SiO}_2$  almost span the entire range of conductivity observed in amorphous solids (actually, the glass with the lowest known conductivity is a K, Ca- $\text{NO}_3$  glass; it is 30% smaller than that of  $\alpha\text{-SiO}_2$ , Ref. 21).

window we used), decreases with increasing  $\text{CN}^-$  concentration. It shifts from 0.7 to 0.2 K as  $x$  increases from 0.25 to 0.70. For  $x=0.05$ , the time dependence is distinctly different from that observed in the glasslike range: The coupling of excess excitations to lattice vibrations is strongly nonlogarithmic and exhibits large effects on the time scale of minutes, in agreement with earlier findings<sup>7</sup> (in the inset of Fig. 9, we only show results for  $t_{\text{exp}}=2$  ms and 10 s; they show time dependence up to 2 K). For  $x \leq 8.5 \times 10^{-4}$ , no time dependence was observed in the time windows 0.01 to 3.0 s at 0.1 K, and 0.001 to 0.2 s, at 1.0 K.<sup>32</sup>

A quantitative analysis of these data will be presented in Sec. V.

## V. DISCUSSION

### A. Analysis of experimental data

In an effort to characterize the centers involved in the glassy excitations found in KBr:KCN crystals, we will next try to extract from the specific-heat anomaly their number density, and subsequently from the thermal conductivity their coupling strength to the phonons.

It is difficult to derive unambiguous information about the vibrational density of states of glasses in the low-

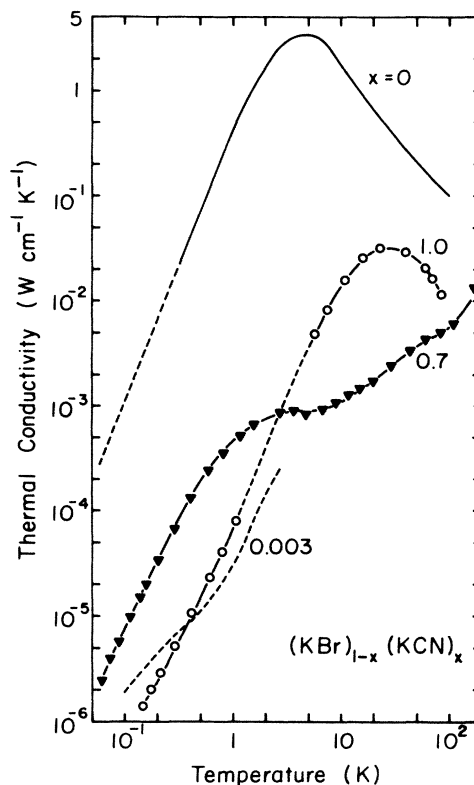


FIG. 6. Thermal conductivity for  $x=0.70$  and for a pure KCN crystal, compared to that of pure KBr and of KBr with a small  $\text{CN}^-$  doping ( $x=0.003$ ). Below the conductivity maximum in KCN, the phonon mean-free path is probably determined by domain wall scattering.

temperature regime from specific-heat measurements. The same problem is encountered in the glasslike crystals  $(\text{KBr})_{1-x}(\text{KCN})_x$ . An inspection of Fig. 7(b) indicates the reasons: Even at the lowest temperatures no indication is found for any simple power-law dependence of the specific heat, which would be evidenced by a straight line in the doubly logarithmic plot of this figure. Furthermore, above  $\approx 1$  K, the  $C_p/C_D$  plot (Fig. 8) shows the onset of the "hump," which probably indicates the presence of some other excitations, different in nature from those seen at the lowest temperatures, but similarly mysterious at this time.<sup>28</sup> Given this difficulty, it was decided to approximate the data below 1 K with a polynomial of the form

$$C_p = c_1 T + (c_D + c_3) T^3, \quad (2)$$

where  $c_1 T$  and  $c_3 T^3$  are the well-known glassy linear and "excess  $T^3$ " specific-heat anomalies, respectively, and  $c_D T^3$  is the Debye phonon specific heat based on elastic data (see Table I). Just as in structural glasses, we do not attach any physical significance to the temperature dependence of the excess  $T^3$  anomaly; this anomaly could, conceivably, be the low-temperature tail of the hump observed at higher temperatures. In Fig. 10 the long-time ( $t \sim 10$  s) specific-heat data are tested against Eq. (2) by plotting  $C_p/T$  versus  $T^2$ . For  $x=0.25, 0.50$ , and  $0.70$ ,

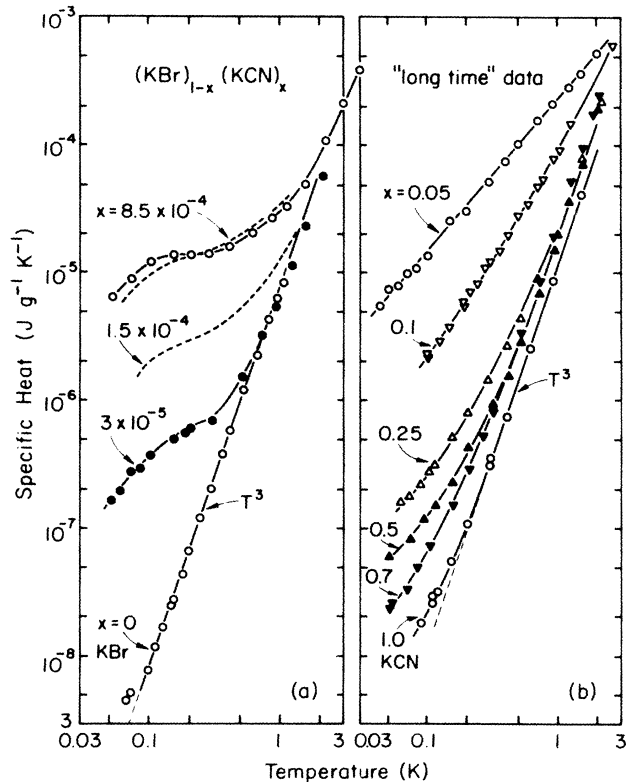


FIG. 7. Low-temperature specific heat of  $(\text{KBr})_{1-x}(\text{KCN})_x$  in the dilute limit (a) and at high  $\text{CN}^-$  concentrations (b). The two dashed curves in (a) had been previously obtained at Cornell [P.P. Peressini (Ref. 61) unpublished; the estimates of the concentrations have been slightly revised, see caption of Fig. 3]. The data in (b) were taken with long measuring times on the order of seconds. For details, see Fig. 9. For  $x=0.10$ , the time was  $\sim 100$  s. Residual impurities are seen in the undoped KBr and KCN below 0.1 and 0.2 K, respectively.

the fits are very good over the entire temperature range 0.05 to  $\sim 1.2$  K, but not for  $x=0.05$  and 0.10. From the straight-line fits, values for  $c_1$  and  $c_D + c_3$  have been determined, see Table I. The values of  $c_1$  lie in the range known for structural glasses.<sup>21</sup> For  $x=0.25$  and 0.70 the values for  $c_3$  indicate an excess  $T^3$  contribution, roughly 50% of the Debye lattice value  $c_D T^3$ . However, for  $(\text{KBr})_{0.5}(\text{KCN})_{0.5}$  the excess  $T^3$  specific heat is only 6% of the Debye value (below 1 K), a negligible difference, considering all errors involved in the comparison. We further note that in Fig. 10 the lowest temperature data for  $x=0.25$  show some curvature, indicating the limit of applicability of Eq. (2).

Other methods of fitting the low-temperature data were also attempted.<sup>13</sup> A slight improvement was obtained by writing the specific heat as

$$C_p = c_\alpha T^\alpha + (c_D + c_3) T^3. \quad (3)$$

For  $x=0.25, 0.50$ , and 0.70 the values of  $\alpha$  giving the best fits for the long-time data are 1.03, 1.00, and 1.08, respectively. A fit of the form

$$C_p = c_\beta T^\beta + c_D T^3 \quad (4)$$

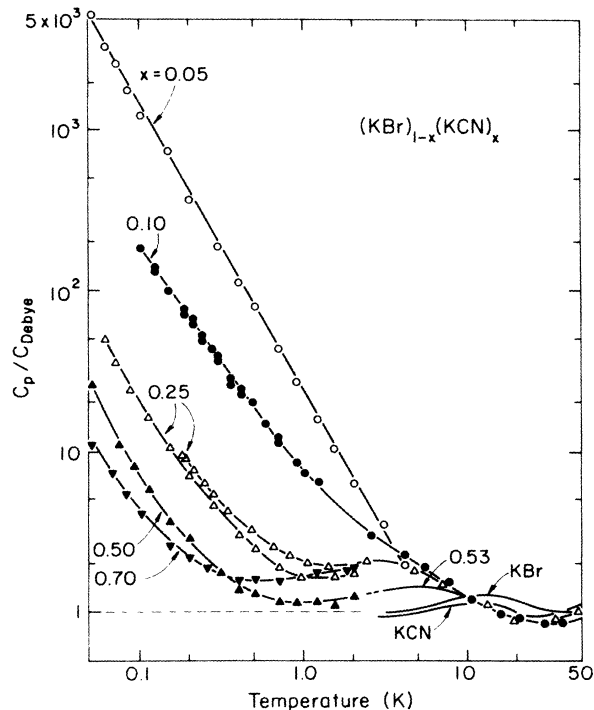


FIG. 8. Same data as shown in Fig. 7(b) but extended to 50 K, and plotted as  $C_p/C_D$ , where  $C_D$  is the specific heat calculated from the Debye integral (see caption of Table I, comments to eighth column). KBr above 3 K, after Berg and Morrison, Ref. 24. Data for  $x=0.53$  above 3 K by Mertz and Loidl, Ref. 27. Two sets of data for  $x=0.25$  are shown, obtained on two different samples, the lower one measured at Berlin, the upper one at Cornell.

was also attempted. Only for  $x=0.50$  was a satisfactory fit obtained. It yielded  $\beta=1.00$ . Since, however,  $c_3$  used in Eqs. (2) and (3) are small (compared to  $c_D$ ) for this sample, the fits obtained with Eqs. (3) and (4) are equivalent. It is thus concluded that with the quality of the data and in particular in the temperature range  $T=0.05$  to  $\approx 1$  K, a fit of the form of Eq. (2) is the most sensible choice.

For a comparison of our data with the standard tunneling model for the linear specific-heat anomaly in structural glasses,<sup>33-36</sup> the usual assumption is made of a spectral distribution  $P(\lambda, \Delta)$  independent of the tunneling parameter  $\lambda$  and of the asymmetry energy  $\Delta$  of the two-level systems (TLS), i.e.,  $P(\lambda, \Delta) = \bar{P}$ . In that case, the specific heat of the TLS is given by<sup>36</sup>

$$C_1 = \frac{1}{\rho} \frac{\pi^2 k_B^2}{12} T \bar{P} \ln(4t/\tau_{\min}), \quad (5)$$

where  $\tau_{\min}$  is the shortest TLS-phonon relaxation time.<sup>35</sup> In order to test the logarithmic time dependence predicted in Eq. (5), we show in Fig. 11 some of the original data, normalized to those obtained at 10 s. If

$$C_p(T_0, t) = C_1(T_0, t) + C_r(T_0), \quad (6)$$

where  $C_r(T_0)$  is the remaining time-independent part of the specific heat at a given temperature  $T_0$ , then we can write

$$\frac{C_p(T_0, t)}{C_p(T_0, 10 \text{ s})} = \frac{C_1(T_0, t) - C_1(T_0, 10 \text{ s}) + C_r(T_0) + C_1(T_0, 10 \text{ s})}{C_p(T_0, 10 \text{ s})} \quad (7)$$

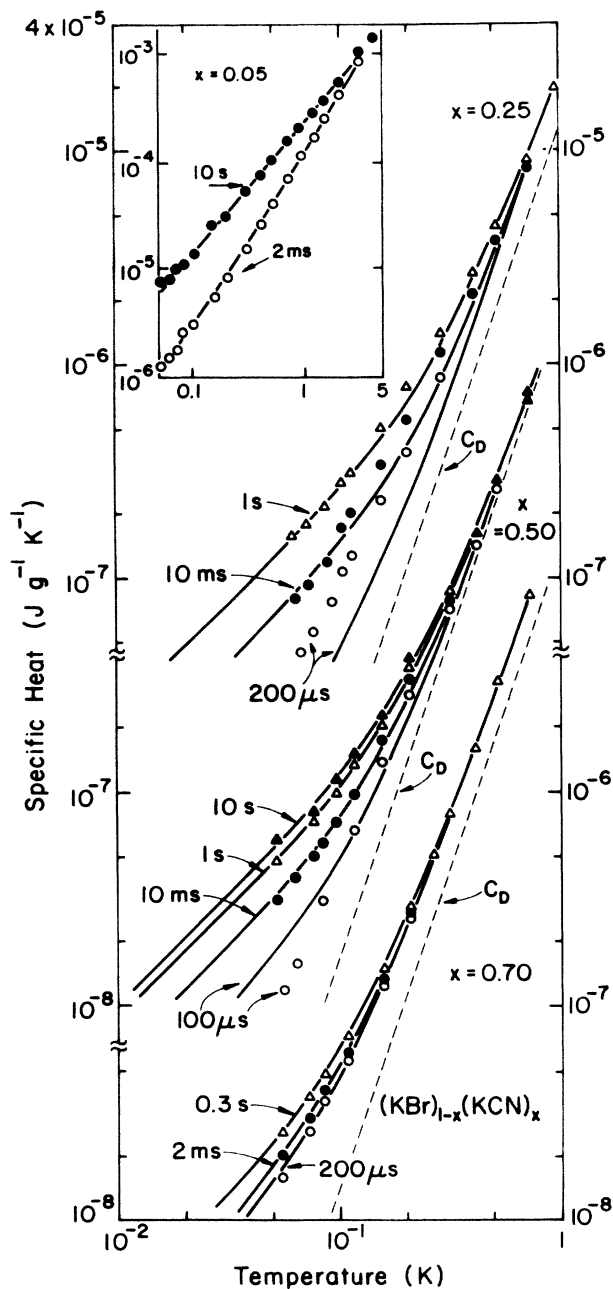


FIG. 9. Specific heat at selected measuring times as indicated. The curves are calculated with Eqs. (2) and (5), using  $c_D$ ,  $c_3$ ,  $c_1$ , and  $\bar{P}$  as listed in Table I. Thus, these curves represent the best fits to all data within the framework of the standard tunneling model. The inset shows the time-dependent specific heat for  $(\text{KBr})_{0.95}(\text{KCN})_{0.05}$ . The time dependence is more pronounced and extends to higher temperatures than for larger  $x$ . These data do not fit the tunneling model; the lines are best fits of a power-law form,  $\propto T^m$  (see below, Fig. 16).

The last two terms in the numerator equal  $C_p(T_0, 10 \text{ s})$ , and hence

$$\frac{C_p(T_0, t)}{C_p(T_0, 10 \text{ s})} = 1 + (\pi^2/12\rho) \frac{k_B^2 T_0 \bar{P} \ln[t/(10 \text{ s})]}{C_p(T_0, 10 \text{ s})} \quad (8)$$

with the second term  $< 0$  for  $t < 10 \text{ s}$ . Thus, a logarithmic time dependence of  $C_1(T_0, t)$  should result in a straight line, if the entire measured specific heat, normalized to some (long-time) value, is plotted versus  $\log t$ , as is indeed observed in Fig. 11. Note that Eq. (8) does not contain  $C_r(T_0)$  and  $\tau_{\min}$ . For  $x=0.50$ , two samples of different thicknesses were measured, and almost five orders of magnitude in measuring time were covered. Good agreement with the tunneling model was also found for  $x=0.25$  and  $0.70$ , although only a somewhat smaller time window was used. From the straight-line best fits, as shown for a few examples in Fig. 11, the density of states  $\bar{P}$  can be determined using Eq. (8). It was found that for any given  $x$ ,  $\bar{P}$  was temperature independent to within the experimental uncertainty of  $\pm 10\%$ . The averages of  $\bar{P}$

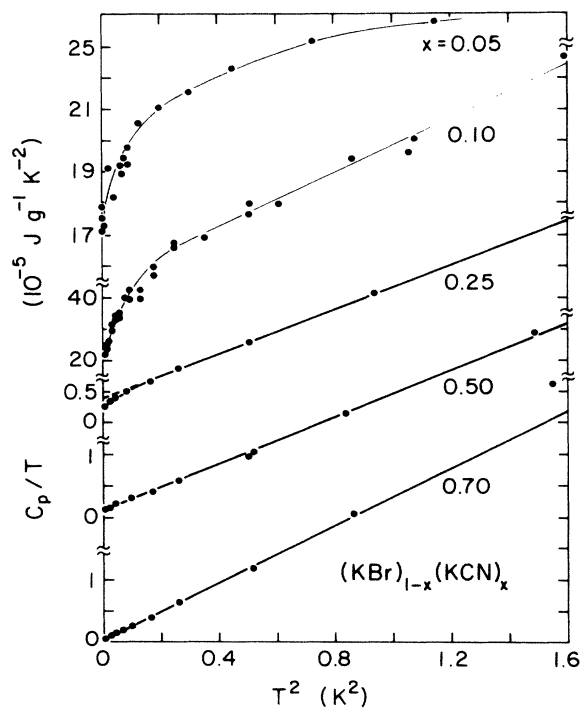


FIG. 10. Test of the applicability of Eq. (2). For  $x=0.25$ ,  $0.50$ , and  $0.70$ ,  $c_1$  and  $c_3$  were determined from intercepts and slopes, respectively, of the straight-line sections of these curves and are listed in Table I. For  $x=0.05$  and  $0.10$ , a linear, glass-like anomaly is not observed. Long time data.

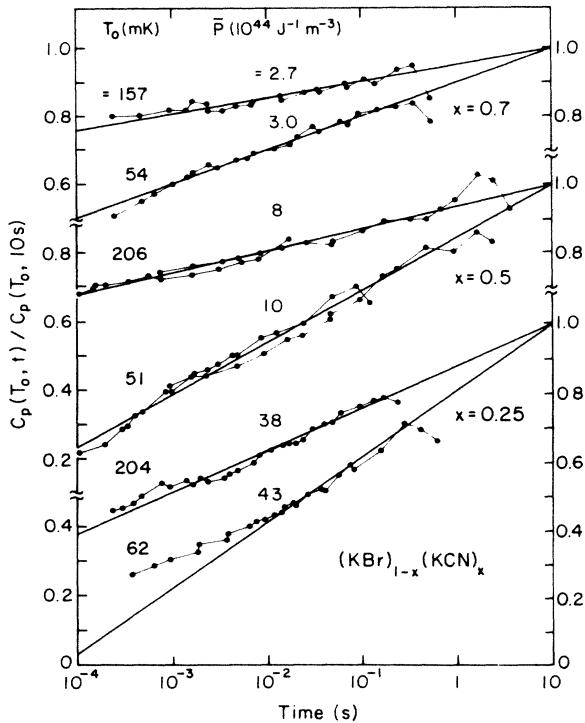


FIG. 11. In the glasslike range of thermal conductivity and specific heat,  $0.25 < x < 0.70$ , the normalized specific heat,  $C_p(T_0, t)/C_p(T_0, 10 \text{ s})$  varies logarithmically with measuring time. For  $x=0.25$ , at the lowest temperatures and shortest measuring times, note a deviation. See text. For  $x=0.50$ , two samples of different thickness were measured.  $\bar{P}$  is determined from the slopes of the straight lines fitted to the data points, see Eq. (8).

are listed in Table I. They agree well with the values obtained from a reanalysis,<sup>37</sup> restricted to the temperature range  $T < 1 \text{ K}$ , of the ultrasonic measurements by Berret *et al.*<sup>9</sup>

We thus conclude that the standard tunneling model describes the low-temperature glasslike specific heat of  $(\text{KBr})_{1-x}(\text{KCN})_x$  rather well. We now show the limitations of this agreement, which are observed for  $x < 0.25$ , and, to some limited degree even for  $x=0.25$ . From  $c_1$  and  $\bar{P}$ ,  $\tau_{\min}$  can be determined with the use of Eq. (5). We obtain  $\tau_{\min} \sim 10 \text{ ns}$ ,  $4 \mu\text{s}$ , and  $0.3 \text{ ms}$  for  $x=0.70$ ,  $0.50$ , and  $0.25$ , respectively. These are obviously approximate values only, since they are independent of temperature, which is unphysical. Nonetheless relaxation times in the range of milliseconds are entirely unreasonable for defects which are strongly coupled to the lattice. Similarly, Berret *et al.*<sup>9</sup> found that they could not fit their ultrasonic data for  $x=0.25$  over the entire temperature range of their measurements by assuming a constant  $\bar{P}$ ; instead, they had to enhance the distribution function  $P(E, \tau)$  at longer relaxation times  $\tau$  [by a weighting factor  $\mu$  which modified the standard distribution function into  $P(E, r, \mu) = \bar{P}r^{-1}(1-r^2)\mu^{-5}$ , where  $r = \tau_{\min}/\tau$ ; in the standard model,  $\mu = 0$ ].

These discrepancies can to some degree be ascribed to

the distribution of barrier heights *assumed* in the standard tunneling model. The modified version of this model, which incorporates the distribution of barrier heights *derived* from dielectric loss measurements, has been developed<sup>10</sup> for  $x=0.50$ . No unphysical values of parameters are necessary in this model; in addition, since the distribution of barrier heights was found to increase with increasing barrier height, it is conceivable that the ultrasonic data can also be explained with this model.

The deviation from a logarithmic time dependence of the specific heat at the lowest temperatures for  $x=0.25$ , shown in Fig. 11 for  $T_0=62 \text{ mK}$ , also disagrees with the standard tunneling model. A similar, though far more pronounced, deviation is observed for  $x=0.05$  (see Fig. 12) for which composition neither the specific heat nor the thermal conductivity show glasslike behavior. Remember also the nonlinear temperature dependence of the long-time specific heat at low temperatures noted above in Fig. 10 for  $x=0.25$ . Thus we conclude that  $x=0.25$  is a borderline case. Its thermal conductivity is certainly glasslike. Its specific heat, however, is beginning to show signs of a "nonglassy" behavior, within the framework of the standard tunneling model.

Turning now to the discussion of the thermal conductivity, we start by considering its magnitude around  $1 \text{ K}$ , (see Figs. 3 and 4). The thermal conductivity of  $(\text{KBr})_{1-x}(\text{KCN})_x$  near  $1 \text{ K}$  is smallest for the relatively modest doping  $x=0.003$ . As  $x$  increases beyond this value, the thermal conductivity increases, so that in the glasslike state, it is more than a factor of ten larger (Fig. 6). The fact that fully disordered, structural glasses have larger thermal conductivities than doped crystals has been noted before, albeit in a comparison of chemically different substances.<sup>38</sup> In the present case, the same increase

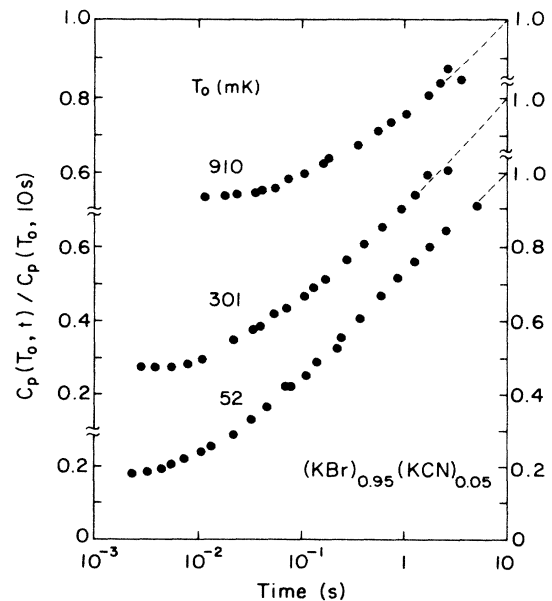


FIG. 12. In the intermediate concentration range,  $x=0.05$  (lower than the glasslike, but higher than the range of single defects), the specific heat does not vary as the logarithm of the measuring time.

of the conductivity, towards that of glasses, has been accomplished by merely increasing the doping level in the crystal. This remarkable observation leads us to restate what we believe to be the crucial question about the universal thermal conductivity of glasses (and now also of glasslike crystals):<sup>38</sup> Why is this conductivity as *large* as it is? If it is determined by defects which scatter the phonons, what limits number density and scattering strength of these defects?

At low temperatures, where resonant interactions between TLS and phonons are dominant, the thermal conductivity is given by<sup>36</sup>

$$\Lambda = \frac{\rho k_B^3 T^2}{6\pi\hbar^2 \bar{P}} \sum_i \frac{v_i}{\gamma_i^2}, \quad (9)$$

where  $v_i$  is the sound velocity of the  $i$ th phonon polarization mode coupled to the TLS via the acoustic coupling-constant (energy)  $\gamma_i$ . In Fig. 13 we show a comparison of the low-temperature thermal-conductivity data of the glasslike crystals with the prediction of Eq. (9), using a power-law fit

$$\Lambda = \tilde{A} T^\delta. \quad (10)$$

For  $x=0.50$  the value for  $\delta$  is very close to 2, whereas for  $x=0.25$  and 0.70 values  $\sim 10\%$  smaller and larger, respectively, are found. A range  $1.8 < \delta < 2.0$  is common for structural glasses below 0.5 K (a recent test of this finding is contained in Ref. 39). An exponent in excess of 2.0, however, has not been observed in structural glasses and requires a comment. It is known that in partly crystallized glasses the conductivity can vary more rapidly with temperature than  $T^2$ , presumably because of additional phonon scattering at the interfaces.<sup>40</sup> The fact that our pure (i.e., undoped) KCN sample does have such a low thermal conductivity (see Fig. 6) may already cast its shadow in the  $x=0.70$  sample. The most likely source of

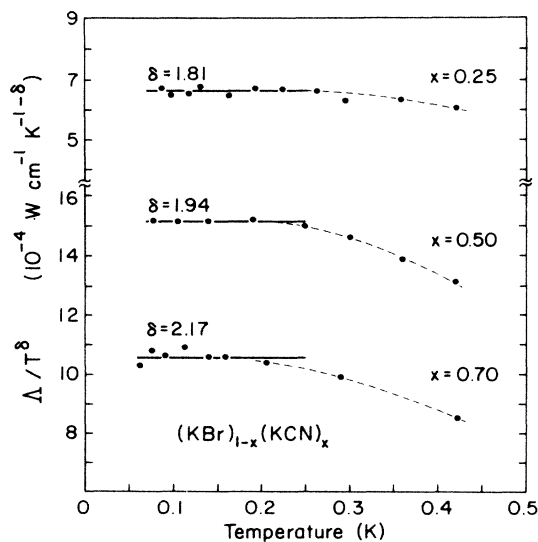


FIG. 13. Best fits of low-temperature thermal conductivity of  $(\text{KBr})_{1-x}(\text{KCN})_x$  in the glasslike compositional range to a power law of the form of Eq. (10),  $\Lambda \propto T^\delta$ .

the scattering in KCN is domain wall scattering. In KCN, Gash and Lüty<sup>41</sup> found ferroelastic domains and secondary structures, suggestive of compound twins. Their length scales were of the order of  $1 \mu\text{m}$ . The thermal conductivity below 10 K of the pure KCN varies approximately as  $T^3$ , its magnitude corresponds to a wavelength independent mean-free path of  $\sim 1 \mu\text{m}$ . We therefore suggest that the additional scattering observed in the  $x=0.70$  sample is also the result of domain wall scattering.

(It must be mentioned, however, that domain wall scattering would not produce the slight knee that can be seen around 1 K in the conductivity curve. Such a structure is more characteristic for resonantly scattering impurities, as it also shown in Fig. 6 for  $x=0.003$  as an example. Such impurities would be noticeable in specific heat. Since no specific-heat measurements were performed on the KCN thermal conductivity sample, resonant scatterers, which would have to have a concentration in excess of 0.1%, though unlikely, cannot be ruled out.)

In order to simplify the discussion, we fitted the low-temperature thermal-conductivity data to

$$\Lambda = AT^2, \quad (11)$$

where the prefactor  $A$  is listed in Table I, again for  $x=0.25, 0.50$ , and  $0.70$ . If we write the sum in Eq. (9) as  $3v_D/\bar{\gamma}^2$ , where  $\bar{\gamma}$  is an averaged coupling constant, the experimental results can be compared to

$$\Lambda = \rho \frac{k_B^3}{2\pi\hbar^2} \frac{v_D}{\bar{P}\bar{\gamma}^2} T^2. \quad (12)$$

We can calculate the average coupling energy  $\bar{\gamma}$  of the TLS to phonons using the values of  $v_D$ ,  $A$ , and  $\bar{P}$  in Table I. For  $x=0.25, 0.50$ , and  $0.70$  we find  $\bar{\gamma}=0.12, 0.18$ , and  $0.48$  eV, respectively, which can be compared again to the ultrasonic results:<sup>37</sup> For  $x=0.25$ ,  $\bar{\gamma}=0.16$  eV, and for  $x=0.50$ ,  $\bar{\gamma}=0.15$  eV, a rather good agreement. Note, however, the large value  $\bar{\gamma}=0.48$  eV for  $(\text{KBr})_{0.3}(\text{KCN})_{0.7}$ . As stated above, an additional scattering mechanism may somewhat affect the thermal conductivity in this sample. However, it cannot account for such a large enhancement of the scattering.

## B. Nature of two-level systems

Although  $(\text{KBr})_{1-x}(\text{KCN})_x$  is crystalline, it is disordered in two ways (see Fig. 14): Firstly, the  $\text{CN}^-$  ions and the  $\text{Br}^-$  ions are randomly distributed over the anion sublattice. This disorder by itself, however, is unlikely to lead to the glasslike behavior. Mixed crystals of alkali halides, for example,  $\text{KBr}:\text{KI}$ , behave like regular, disordered crystals.<sup>42</sup> Furthermore, glasslike behavior has also been found in mixed crystals of alkali cyanides, i.e., crystals containing no topological disorder in the anion sublattice, as we have shown by measuring the thermal conductivity of a single crystal  $(\text{KCN})_{0.25}(\text{NaCN})_{0.75}$  (see Fig. 15). Its temperature dependence and magnitude are also indistinguishable from that of a structural glass, e.g., silica.

Secondly, in mixed alkali halide-alkali cyanide and in

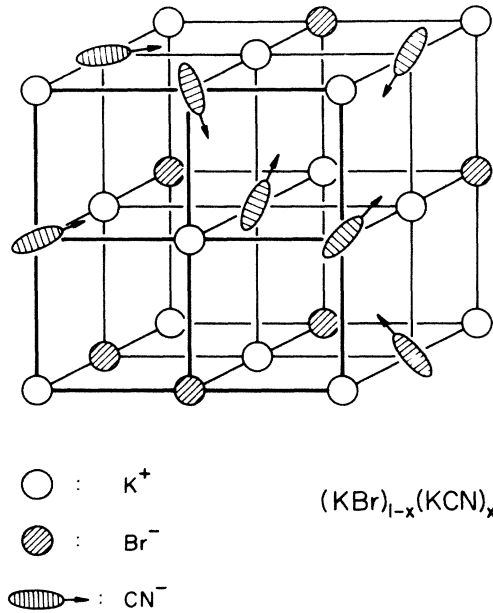


FIG. 14. Lattice model of cubic (KBr)<sub>1-x</sub>(KCN)<sub>x</sub>.

mixed alkali cyanide crystals, one other common source of disorder can be found: The CN<sup>-</sup> molecule ions are disordered with respect to their orientations in the cubic lattice. At high temperatures, this orientational disorder results from a dynamical process, which can be described by thermally activated CN<sup>-</sup> rotations interacting with the phonon system, whereas at low temperatures, i.e.,  $T < 5$  K, the CN<sup>-</sup> ions form a static orientational glass.<sup>5,43</sup> For example, in the compositional range  $x < 0.56$ , and below a

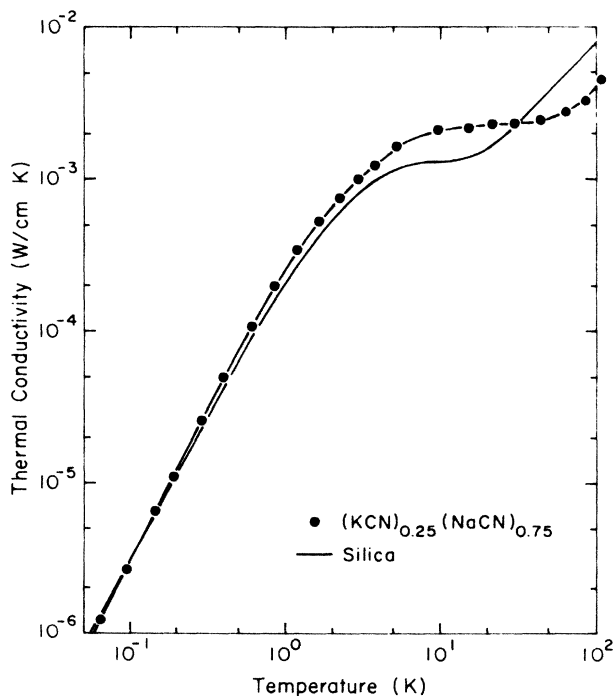


FIG. 15. Thermal conductivity of single crystal (KCN)<sub>0.25</sub>(NaCN)<sub>0.75</sub>, compared to that of  $\alpha$ -SiO<sub>2</sub>.

certain, frequency-dependent, freezing temperature  $T_F(x, \omega)$ , (KBr)<sub>1-x</sub>(KCN)<sub>x</sub> freezes into an orientational glass state,<sup>44</sup> in which the CN<sup>-</sup> axes are randomly oriented, as also shown schematically in Fig. 14. An orientational glass state has also been reported in (KCN)<sub>1-x</sub>(NaCN)<sub>x</sub> for  $0.10 < x < 0.85$ .<sup>44,45</sup> One might thus assume that this orientational glass state gives rise to the glasslike low-energy properties. However, this picture cannot be correct either since glasslike thermal properties are also observed for  $x=0.70$  in (KBr)<sub>1-x</sub>(KCN)<sub>x</sub>, for which composition orientational long-range order has been established.<sup>20,44</sup> In addition, dielectric loss measurements have shown that the low-frequency dielectric loss peak continuously broadens into a glassy behavior as  $x$  decreases from pure KCN ( $x=1$ ) to (KBr)<sub>0.5</sub>(KCN)<sub>0.5</sub>.<sup>5,46,47</sup> Thus, both the glassy low-temperature thermal properties and the glassy low-frequency dielectric behavior appear to be insensitive to the presence of long-range crystalline orientational order. We must therefore conclude that neither type of disorder discussed above is responsible for the glasslike thermal properties in (KBr)<sub>1-x</sub>(KCN)<sub>x</sub>.

Recently, it has been argued that both the time-dependent specific heat and the dielectric loss peak can be explained in terms of 180° electric dipole reorientations of the CN<sup>-</sup> ions, i.e., that the glassy properties result from a tunneling and/or thermally activated motion of individual cyanide ions through (or above) angular orientation barriers provided by a quadrupolar mean field of elastic CN<sup>-</sup>-CN<sup>-</sup> interactions.<sup>8,10</sup> It has been shown that, while at high temperatures all CN<sup>-</sup> ions can reorient in an electric field, at temperatures below 1 K only a very small fraction, of the order of  $10^{-5}$  for  $x=0.50$ , can reorient by tunneling. It is this small fraction of individual ions that causes the glasslike excitations in (KBr)<sub>1-x</sub>(KCN)<sub>x</sub>.

Pursuing this picture, we first consider the thermal conductivity. The strain coupling of isolated CN<sup>-</sup> ions in a KBr crystal to a shear wave in the  $\langle 100 \rangle$  direction is given by<sup>4,48</sup>

$$\gamma \langle 100 \rangle = \frac{1}{3}(\lambda_1 - \lambda_2)V_0c_{44} = 0.15 \text{ eV}, \quad (13)$$

where  $V_0$  is the volume of the primitive unit cell ( $70 \text{ \AA}^3$  in KBr), and  $c_{44}$  is the shear modulus (see Table I); the elastic dipole shape factor  $(\lambda_1 - \lambda_2) = 0.2$  is taken from Beyeler.<sup>4</sup> This coupling energy is very close to the  $\bar{\gamma} = 0.12$  and  $0.18$  eV for (KBr)<sub>0.75</sub>(KCN)<sub>0.25</sub> and (KBr)<sub>0.5</sub>(KCN)<sub>0.5</sub>, respectively, calculated by fitting our thermal-conductivity results. The much larger value of  $\bar{\gamma}$  for  $x=0.70$ , however,  $0.48$  eV, demonstrates the limits of the single-ion picture.

Another test of the picture can be made with measurements of the low-temperature dielectric constant. According to the tunneling model, the real part of the dielectric constant is given by<sup>49</sup>

$$\Delta\kappa = \kappa(T) - \kappa(T_0) = [2/(3\epsilon_0)](p_0)^2\bar{P} \ln(T/T_0), \quad (14)$$

where  $p_0$  is the static electric dipole moment of the tunneling defects, and  $T_0$  is some reference temperature. Low-temperature measurements have been reported only for  $x \leq 0.2$ .<sup>7,50</sup> However,  $x=0.20$  is at least close to the range in which the low-temperature glasslike properties

have been observed. We have extrapolated  $\bar{P}(x)$  from Table I to  $x=0.20$ , and obtained  $\bar{P}\approx 50\times 10^{44}\text{ J}^{-1}\text{ m}^{-3}$ . An analysis of the dielectric data using Eq. (14) leads to a permanent dipole moment  $p_0=(0.15\pm 0.02)$  Debye.<sup>51</sup> For isolated  $\text{CN}^-$  ions in KBr,  $p_0=0.5$  Debye has been reported,<sup>23</sup> three times as large as obtained here. This result, although certainly preliminary, also fails to support the single-ion picture. Clearly, more extensive dielectric measurements are needed, including a study of the anisotropy, which exists in the dilute limit, but should be absent in the limit of orientational disorder.

We now turn to the question of whether the interaction leading to the glasslike excitations is electric or elastic in nature. Recently, Volkman *et al.*<sup>52</sup> have presented evidence for either type of interaction. Below, we consider the changeover of the low-temperature specific heat of the individual tunneling ions to that of the glasslike excitations. Figure 16 summarizes the (long-time) specific heat of  $(\text{KBr})_{1-x}(\text{KCN})_x$  in the intermediate concentration range,  $0.01 < x < 0.10$ . The low-temperature data can be

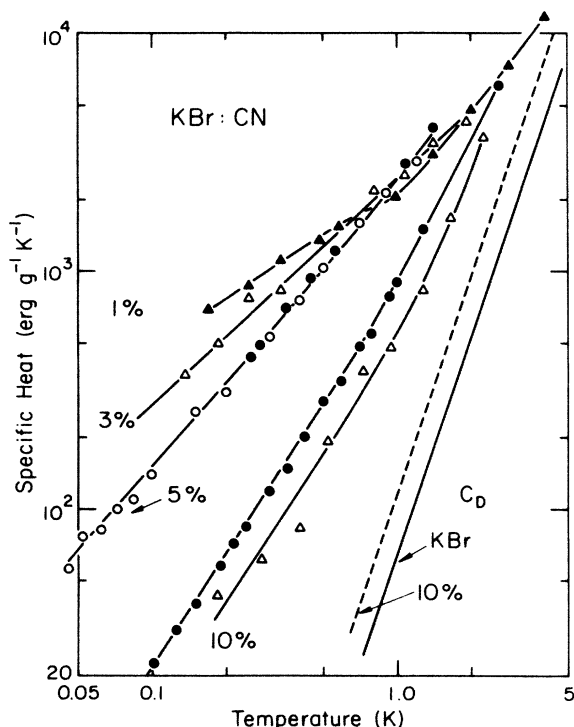


FIG. 16. Specific heat of  $(\text{KBr})_{1-x}(\text{KCN})_x$  in the intermediate composition range of  $x$  (1 to 10%), measured on long-time scales. Triangles: Moy *et al.*, Refs. 7 and 50, time scale  $\sim 100$  s. Open circles: this work, measurements at Berlin, time scale 10 s. Solid circles: This work, measurements at Cornell; time scale 100 s. Note that in view of the different time scales used for the two measurements of  $x=0.05$ , the excellent agreement is slightly fortuitous. Based on the time-dependent measurements, see Fig. 12, one would expect the Cornell data to lie  $\sim 20\%$  above the Berlin data. We attribute this kind of variation to fluctuation in the sample composition, etc., and to measuring errors caused mainly by the pronounced time dependence at long measuring times. See also the variations for  $x=0.10$ , Cornell versus Illinois. Debye specific heats  $C_D$  (Table I) as measured for KBr, and as calculated for  $x=0.10$ .

described fairly well by power laws,  $C_p \propto T^m$ , with the exponent  $m$  given by 0.68 for  $x=1\%$ , 0.96 for 3%, 1.2 for 5%, and 1.6 for 10%. Thus, as  $x$  increases,  $C_p$  changes from a rather weak-temperature dependence [as also seen in the dilute limit in this temperature range, see Fig. 7(a)], to an increasingly more rapid temperature dependence, with  $m$  approaching the value of  $\frac{3}{2}$  [as also noted previously in KCl:OH (Ref. 53)]. A further increase of  $x$  leads to a change towards the glasslike, linear specific-heat anomaly. The transition from the specific heat of the dilute limit to that of the glasslike limit is further illustrated in Fig. 17, where the excess specific heat,  $C_p - C_D$ , of  $(\text{KBr})_{1-x}(\text{KCN})_x$  at 0.1 K is plotted for the entire range of  $x$  investigated (including recent data by Dobbs *et al.*, Ref. 54). For  $x < 0.1\%$ , a rise in linear proportion with  $x$  indicates the absence of interactions between the  $\text{CN}^-$  ions. For  $x \geq 0.03$ , the long-time excess specific heat varies rather closely as  $x^{-2}$ . This particular dependence on  $x$  is somewhat fortuitous in the concentration region  $0.03 < x < 0.25$ , and would not be found at different temperatures, because of the variation of the power-law ex-

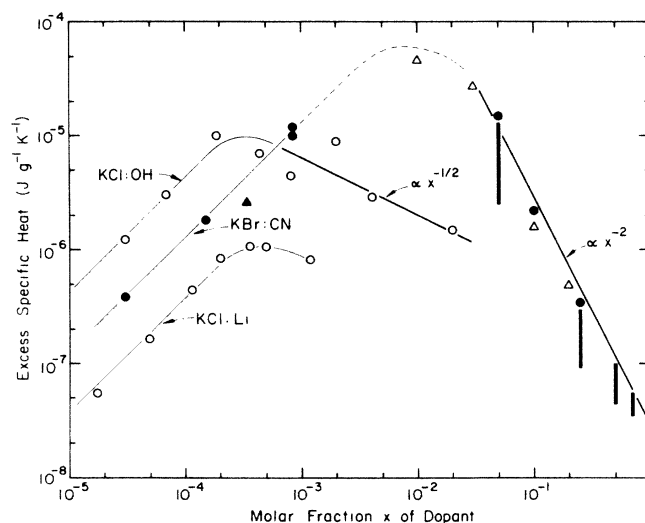


FIG. 17. Measured specific heat minus Debye specific heat (Table I) at 0.1 K. KCl:OH (open circles) from Refs. 53, 56, and 57, and KCl:Li (open circles) from Refs. 55 and 56; all measurements had been taken on 10–100 s time scales.  $(\text{KBr})_{1-x}(\text{KCN})_x$ : closed circles: this work, long-time measurements (10–100 s); open triangles: Ref. 7, solid triangle: Ref. 54, with the measuring times not given, but estimated to be 10–100 s. For  $x \geq 0.05$ , the vertical bars indicate our time-dependent specific heat measured between 1 ms (low end of bar) and 10 s (upper end). The straight lines through the data in the low  $x$  range  $x < 10^{-4}$  indicate a scaling of the specific-heat anomaly with  $x$ , i.e., the absence of defect-defect interactions. These begin to show up at  $x \sim 3 \times 10^{-4}$  for  $\text{OH}^-$  and  $\text{Li}^+$ , but for  $\text{CN}^-$  only above  $10^{-3}$ . The dashed curve connecting the high- $x$  and the low- $x$  data for  $(\text{KBr})_{1-x}(\text{KCN})_x$  is drawn to visualize where  $\text{CN}^-$ - $\text{CN}^-$  interactions may be expected to set in at 0.1 K. The solid line through the  $\text{OH}^-$  data above  $x = 10^{-3}$  varies as  $x^{-1/2}$ , as first suggested by Fiory (Ref. 53). The solid line, labeled  $x^{-2}$ , is an empirical relation observed in this investigation.

ponent  $m$  for  $x < 0.25$ . Nevertheless, the rapid decrease of the excess long-time specific heat, as  $x$  increases, and the approach to a  $x^{-2}$  dependence for  $x > 0.25$ , are generally correct. For short measuring times (1 ms in Fig. 17), the specific heat shows a different behavior.

Only in the dilute limit is the shape of the Schottky specific-heat anomaly of the tunneling states of impurities in alkali halides independent of concentration, i.e., for mole fractions  $x$  typically less than  $10^{-3}$  or  $10^{-4}$ , as has been shown for KCl:Li,<sup>55,56</sup> KCl:OH,<sup>56,57</sup> and RbCl:OH.<sup>53</sup> For KCl:Li and KCl:OH, interactions set in at a limiting mole fraction approximately  $2 \times 10^{-4}$ , as seen in Fig. 17. Fiory has shown that interaction effects seen in dielectric measurements in these crystals are the result of electric dipole interactions,<sup>53</sup> and since these effects occurred at the same temperatures at which interaction was seen in specific heat (for a given concentration), he concluded that the latter effects, too, were the result of electric, and not of stress interactions.

For  $(\text{KBr})_{1-x}(\text{KCN})_x$ , the excess specific heat at 0.1 K rises linearly with  $x$  up to at least  $x = 10^{-3}$ , and probably to even higher values of  $x$ , if we interpolate to the larger  $x$  values as has been done in Fig. 17. According to Fiory's estimates, one would not expect to notice electric dipole interactions at 0.1 K for  $\text{CN}^-$  number densities  $m$  less than  $1.5 \times 10^{20} \text{ cm}^{-3}$ , i.e.,  $x \sim 1\%$ . Fiory did not find any evidence for interactions in KCl:CN for  $n = 4.2 \times 10^{19} \text{ cm}^{-3}$  ( $x = 2.6 \times 10^{-3}$ ), the highest concentration he investigated. Depending on how one wishes to interpolate the data for  $(\text{KBr})_{1-x}(\text{KCN})_x$  in Fig. 17, one may determine the critical concentration to be  $\sim 0.5\%$ , not far from the value based on Fiory's estimate. Quadrupole stress interactions, on the other hand, would be expected to occur at a roughly 30 times smaller  $x$ , i.e., at  $x = 2 \times 10^{-4}$ , according to estimates by Peressini *et al.*<sup>56</sup> Thus it appears that the maximum in the specific heat seen in  $(\text{KBr})_{1-x}(\text{KCN})_x$  in Fig. 17 is the result of electric, and not of elastic interactions.

We now turn to the rapid drop of the specific heat for  $x > 0.05$ , which varies approximately proportional to  $x^{-2}$ . Klein *et al.*<sup>58</sup> have argued that interacting dipoles would lead to a concentration-independent linear specific heat at high concentrations, while Fiory suggested a variation with  $n^{-1/2}$  (i.e.,  $x^{-1/2}$ ), in analogy with ferromagnetic spin waves.<sup>53</sup> See also the recent work by Moy *et al.*<sup>59</sup>

One further complexity should be mentioned. In KCl, the Schottky anomaly of the  $\text{CN}^-$  tunneling states is quite narrow for the smallest  $n$  ( $4.4 \times 10^{17} \text{ cm}^{-3}$ ), but broadens significantly as  $n$  increases.<sup>56</sup> Consequently, the specific heat of KCl:CN at a fixed temperature does not increase linearly with  $x$  even at the smallest  $x$ . This broadening could conceivably be the result of elastic interactions. In KBr, the Schottky anomaly is broad even at low  $x$  (Fig. 7),<sup>22</sup> and changes its shape only very little as long as  $x < 10^{-3}$ . As a result, the specific heat rises linearly with  $x$  (see Fig. 17), but an important mechanism of interaction between the ions may be hidden in this case.

### C. Thermal conductivity above 1 K

The glasslike thermal conductivity of  $(\text{KBr})_{1-x}(\text{KCN})_x$ , which has been observed for

$0.25 \leq x \leq 0.70$ , is not restricted to the low-temperature range covered by the tunneling model but extends to the highest temperature of our measurements (100 K) (see Fig. 4). (A peculiar abrupt change of the conductivity observed in our earlier work,<sup>6</sup> has not been reproduced<sup>13</sup> and should be ignored at this time.) The thermal conductivity of  $(\text{KBr})_{1-x}(\text{KCN})_x$  in a *structurally* amorphous form is not known since such a substance has never been produced, but we can estimate its magnitude by using the gas-kinetic formula of thermal conductivity,  $\Lambda = (\frac{1}{3}) C_v l v$ . For simplicity, we use the data for KBr,  $C \approx C_p = 10.3 \text{ cal mol}^{-1} \text{ K}^{-1}$  at 100 K,  $v \approx v_D = 1.88 \times 10^3 \text{ m s}^{-1}$  (Table I), and for  $l$  we use the average interatomic separation (one-half of the unit-cell dimension)  $l = 3.3 \text{ \AA}$ . The calculated  $\Lambda = 2 \times 10^{-3} \text{ W cm}^{-1} \text{ K}^{-1}$  is close to the measured value (at 100 K), considering the crudeness of the model. It therefore seems reasonable to conclude that in the glasslike state, crystalline  $(\text{KBr})_{1-x}(\text{KCN})_x$  has a conductivity close to the theoretical expectation of the minimum thermal conductivity,<sup>60</sup> according to which the heat diffuses, in a random walk, from atom to atom at temperatures above  $\sim 50 \text{ K}$ .

The actual mechanism by which the heat is transported in glasses in the temperature region of the plateau and above continues to be a matter of controversy.  $(\text{KBr})_{1-x}(\text{KCN})_x$ , which is so far the only crystalline system in which the transition from a crystalline, high, to a glasslike, low thermal conductivity has been accomplished by varying the mixing ratio, should be an ideal substance to study the origin of this minimum thermal conductivity. We believe, however, that this requires also measurements above 100 K. These are presently under way.

## VI. CONCLUSION

While by now a number of disordered crystalline systems have been identified which display glasslike low-temperature properties,<sup>1</sup>  $(\text{KBr})_{1-x}(\text{KCN})_x$  is the only system in which the transition from crystalline to glasslike behavior has been studied in systematically prepared mixed crystals. These crystals have been used in an attempt to unravel some of the mysteries of the vibrational excitations in structurally amorphous solids. As the KCN molar fraction  $x$  increases, the individual  $\text{CN}^-$  tunneling ions show increasingly stronger interactions. Thus, the low-temperature specific-heat anomaly goes through a maximum with increasing  $x$ , and changes its shape towards a glasslike specific heat which varies linearly with temperature. Simultaneously, the thermal conductivity below  $\sim 10 \text{ K}$  goes through a *minimum*, and *increases* towards that typical of all amorphous solids. In the compositional range in which glasslike thermal properties are observed,  $x = 0.25$  to  $x = 0.70$ , the specific heat displays a logarithmic time dependence which has been studied over five orders of magnitude in time. The standard tunneling model proposed for structural glasses has been used to describe the low-temperature properties in the glasslike state. The spectral density  $\bar{P}$  decreases by over one order of magnitude as  $x$  increases from 0.25 to 0.70. Very remarkably, the thermal conductivity shows only a very small variation.

No obvious correlation between the glasslike properties and the phase diagram for  $(\text{KBr})_{1-x}(\text{KCN})_x$  can be detected: The glasslike behavior is not restricted to the compositional range in which the  $\text{CN}^-$  ions form an orientational glass, which is believed to extend from  $x=0.56$  to the neighborhood of 0.01; it is also found for  $x=0.70$ , for which composition long-range order of the  $\text{CN}^-$  ions exists. The picture that the low-energy glasslike excitations are tunneling states of a small fraction of the  $\text{CN}^-$  ions which retain their quasirotational mobility, which has been successful in correlating the dielectric loss data and the low-temperature specific heat,<sup>10</sup> leads to somewhat unrealistic electric and elastic coupling energies for  $x=0.70$ , and thus will also need some modifications.

At low concentrations, interactions occurring at  $x < 0.05$  do not result in the same low-temperature thermal properties as are observed in all structural glasses.

The interaction mechanism which leads to the freezing of the  $\text{CN}^-$  ions is not well understood. The onset of the freezing, as  $x$  increases beyond  $\approx 10^{-3}$ , coincides with the concentration at which electric dipole interaction is ex-

pected to set in. Whatever the interaction mechanism, it is most remarkable that it should lead to the same thermal properties as they exist in all structural glasses. It is the generality of the phenomenon, which now has also been extended to these disordered crystals, which continues to present the greatest puzzle.

#### ACKNOWLEDGMENTS

Stimulating discussion with J. P. Sethna, J. F. Berret, and J. VanCleve are gratefully acknowledged. One of the authors (M.M.) acknowledges the hospitality extended to him by the Laboratory of Atomic and Solid State Physics at Cornell University and also the financial support by the Deutsche Forschungsgemeinschaft (Bonn, Germany) during his stay there. This work was supported at Cornell University in part by the National Science Foundation, Grant No. DMR-84-17557, and the Materials Science Center, and in Berlin by the Deutsche Forschungsgemeinschaft.

\*Present address: Department of Geology, University of Maine, Orono, ME 04469.

†Present address: Hahn-Meitner Institut für Kernforschung, D-1000 Berlin 39, Federal Republic of Germany.

<sup>1</sup>See, e.g., A. C. Anderson, *Phase Transitions* 5, 301 (1985); R. O. Pohl, J. J. De Yoreo, M. Meissner, and W. Knaak, in *Physics of Disordered Materials*, edited by D. Adler, H. Fritzsche, and S. Ovshinsky (Plenum, New York, 1985), p. 529.

<sup>2</sup>V. Narayanamurti, *Phys. Rev. Lett.* 13, 693 (1964).

<sup>3</sup>W. D. Seward and V. Narayanamurti, *Phys. Rev.* 148, 463 (1966).

<sup>4</sup>H. U. Beyeler, *Phys. Rev. B* 11, 3078 (1975).

<sup>5</sup>F. Lüty, in *Defects in Insulating Crystals*, edited by V. M. Tuckevich and K. K. Swartz (Springer-Verlag, Berlin, 1981), p. 69.

<sup>6</sup>J. J. De Yoreo, M. Meissner, R. O. Pohl, J. M. Rowe, J. J. Rush, and S. Susman, *Phys. Rev. Lett.* 51, 1050 (1983).

<sup>7</sup>D. Moy, J. N. Dobbs, and A. C. Anderson, *Phys. Rev. B* 29, 2160 (1984).

<sup>8</sup>M. Meissner, W. Knaak, J. P. Sethna, K. S. Chow, J. J. De Yoreo, and R. O. Pohl, *Phys. Rev. B* 32, 6091 (1985).

<sup>9</sup>J. F. Berret, P. Doussineau, A. Levelut, M. Meissner, and W. Schön, *Phys. Rev. Lett.* 55, 2013 (1985).

<sup>10</sup>J. P. Sethna and K. S. Chow, *Phase Transitions* 5, 317 (1985).

<sup>11</sup>E. Meyer, *Chemistry of Hazardous Materials* (Prentice-Hall, Englewood Cliffs, 1977).

<sup>12</sup>J. M. Rowe (private communication).

<sup>13</sup>For details, see J. J. De Yoreo, Ph.D. thesis, Cornell University, 1985 (unpublished).

<sup>14</sup>R. Krüger, M. Meissner, J. Mimkes, and A. Tausend, *Phys. Status Solidi A* 17, 471 (1973).

<sup>15</sup>A. K. Raychaudhuri and R. O. Pohl, *Phys. Rev. B* 25, 1310 (1982).

<sup>16</sup>For details, see W. Knaak, Ph.D. thesis, Technical University, Berlin, 1985 (unpublished).

<sup>17</sup>W. Knaak and M. Meissner, in *Phonon Scattering in Condensed Matter V*, edited by A. C. Anderson and J. P. Wolfe (Springer, Berlin, 1986), p. 174.

<sup>18</sup>J. F. Berret, Thèse d'Etat, Université de Montpellier, France, 1987 (unpublished).

<sup>19</sup>See G. A. Alers, in *Physical Acoustics* edited by P. W. Mason (Academic, New York, 1965), Vol. III B, p. 1.

<sup>20</sup>K. Knorr and A. Loidl, *Phys. Rev. B* 31, 5387 (1985).

<sup>21</sup>R. B. Stephens, *Phys. Rev. B* 13, 852 (1976).

<sup>22</sup>R. L. Pompei and V. Narayanamurti, *Solid State Commun.* 6, 645 (1968).

<sup>23</sup>V. Narayanamurti and R. O. Pohl, *Rev. Mod. Phys.* 42, 201 (1970).

<sup>24</sup>W. T. Berg and J. A. Morrison, *Proc. R. Soc. London, Ser. A* 242, 467 (1967).

<sup>25</sup>W. Knaak and M. Meissner, in *Proceedings of the Seventeenth International Low Temperature Conference*, edited by U. Eckern *et al.* (North-Holland, Amsterdam, 1984), p. CR6.

<sup>26</sup>B. N. Brockhouse and P. K. Iyengar, *Phys. Rev.* 111, 747 (1958).

<sup>27</sup>B. Mertz and A. Loidl, *J. Phys. C* 18, 2843 (1985).

<sup>28</sup>R. O. Pohl and E. T. Swartz, *J. Non-Cryst. Solids* 76, 117 (1985).

<sup>29</sup>M. T. Lopenen, R. C. Dynes, V. Narayanamurti, and J. P. Garno, *Phys. Rev. Lett.* 45, 457 (1980); *Phys. Rev. B* 25, 1161 (1982); 25, 4310 (1982).

<sup>30</sup>M. Meissner and K. Spitzmann, *Phys. Rev. Lett.* 46, 265 (1981); W. Knaak and M. Meissner, in *Phonon Scattering in Condensed Matter*, edited by W. Eisenmenger *et al.* (Springer, Berlin, 1984), p. 416.

<sup>31</sup>J. Zimmermann and G. Weber, *Phys. Rev. Lett.* 46, 661 (1981).

<sup>32</sup>We mention in passing that we did observe a rather rapid dropoff of the specific heat with decreasing measuring time in the  $x = 3 \times 10^{-5}$  sample, setting in abruptly below 0.2 K on a 100- $\mu$ s time scale. We believe that this effect is due to the decoupling of accidental lattice defects; the most likely accidental impurity is  $\text{NCO}^-$ , see Ref. 3. For a discussion of an apparent time-dependent specific heat in nominally pure crystals, see Refs. 17 and 25.

<sup>33</sup>P. W. Anderson, B. I. Halperin, and C. M. Varma, *Philos. Mag.* 25, 1 (1972).

<sup>34</sup>W. A. Phillips, *J. Low Temp. Phys.* 7, 351 (1972).

<sup>35</sup>J. Jäckle, *Z. Phys.* 257, 212 (1972).

- <sup>36</sup>J. L. Black, *Phys. Rev. B* **17**, 2740 (1978).
- <sup>37</sup>J. F. Berret and M. Meissner, in *Phonon Scattering in Condensed Matter V*, edited by A. C. Anderson and J. P. Wolfe (Springer, Berlin, 1986), p. 83.
- <sup>38</sup>R. C. Zeller and R. O. Pohl, *Phys. Rev. B* **4**, 2029 (1971).
- <sup>39</sup>A. K. Raychaudhuri, Ph.D. thesis, Cornell University, 1980; Cornell Materials Science Center Report No. 4284 (unpublished).
- <sup>40</sup>R. C. Zeller, M. S. thesis, Cornell University, 1971; Cornell Material Science Center Report No. 1453 (unpublished).
- <sup>41</sup>P. Gash and F. Lüty, *Microscopy* **140**, 351 (1985).
- <sup>42</sup>B. D. Nathan, L. F. Lou, and R. H. Tait, *Solid State Commun.* **19**, 615 (1976).
- <sup>43</sup>J. M. Rowe, J. J. Rush, D. G. Hinks, and S. Susman, *Phys. Rev. Lett.* **43**, 1158 (1979); K. H. Michel and J. M. Rowe, *Phys. Rev. B* **22**, 1417 (1980).
- <sup>44</sup>F. Lüty and J. Ortiz-Lopez, *Phys. Rev. Lett.* **50**, 1289 (1983).
- <sup>45</sup>T. Schröder, A. Loidl, K. Knorr, and J. K. Kjems, in *Phonon Physics*, edited by J. Kollar *et al.* (World Scientific, Philadelphia, 1985), p. 111; A. Loidl, T. Schröder, R. Bohmer, K. Knorr, J. K. Kjems, and R. Born, *Phys. Rev. B* **34**, 1238 (1986).
- <sup>46</sup>N. O. Birge, Y. H. Jeong, S. R. Nagel, S. Battacharya, and S. Susman, *Phys. Rev. B* **30**, 2306 (1984).
- <sup>47</sup>J. P. Sethna, S. R. Nagel, and T. V. Ramakrishnan, *Phys. Rev. Lett.* **53**, 2489 (1984).
- <sup>48</sup>Since  $c_{11} \gg c_{44}$ , those modes for which  $c_{11}$  is contained in their  $\gamma$  are too strongly coupled to the  $\text{CN}^-$  ions to contribute to the heat conduction, and only those terms containing  $c_{44}$  alone are of importance.
- <sup>49</sup>M. von Schickfus and S. Hunklinger, *J. Phys. C* **9**, L439 (1976). Their Eq. (2) contains a misprint: The denominator contains a 2, instead of the correct 3. In the standard tunneling model, the product  $(\rho_0)^2 \bar{P}$  equals  $(\mu')^2 n_0$ , where  $\mu'$  is the induced dipole moment, and  $n_0$  the density of states of the tunneling centers. See also W. A. Phillips, *Philos. Mag. B* **43**, 747 (1981).
- <sup>50</sup>D. Moy, Ph.D. thesis, University of Illinois, Urbana, 1983 (unpublished).
- <sup>51</sup>The dielectric constants  $\kappa$  were calculated from the measured capacitances  $C$  measured by Moy, Ref. 50, assuming  $C = \kappa \epsilon_0 A/d$ , where  $A = 2.82 \text{ cm}^2$  and  $d = 0.103 \text{ cm}$  are sample area and thickness, respectively, and  $\epsilon_0 = 8.9 \times 10^{-12} \text{ As/Vm}$  (practical units). Because of expected errors in the geometry, Moy (p. 91) estimated the error in  $A/d$  to be roughly  $\pm 50\%$ . However, from his value of  $C(T_0) = 12.76695 \text{ pF}$  one calculates  $\kappa(T_0) = 5.3$ , using the above formula. For  $x = 0.2$ , Lüty (Ref. 5, Fig. 17) gives  $\kappa \approx 4.9$  below 5 K. Thus, we believe the error in  $\kappa$  to be no more than 10% for this sample. For the measuring frequency 10 kHz,  $T_0 = 0.1 \text{ K}$ , and for 81 kHz,  $T_0 = 0.15 \text{ K}$ . The value of  $p_0$  determined by us earlier (Ref. 8) is incorrect because of problems we had with the Gaussian system of units.
- <sup>52</sup>U. G. Volkmann, R. Böhmer, A. Loidl, K. Knorr, U. T. Höchli, and S. Haussühl, *Phys. Rev. Lett.* **56**, 1716 (1986).
- <sup>53</sup>A. T. Fiory, *Phys. Rev. B* **4**, 614 (1970).
- <sup>54</sup>J. N. Dobbs, M. C. Foote, and A. C. Anderson, *Phys. Rev. B* **33**, 4178 (1986).
- <sup>55</sup>J. P. Harrison, P. P. Peressini, and R. O. Pohl, *Phys. Rev.* **171**, 1037 (1968).
- <sup>56</sup>P. P. Peressini, J. P. Harrison, and R. O. Pohl, *Phys. Rev.* **182**, 939 (1969).
- <sup>57</sup>J. J. De Yoreo, R. O. Pohl, J. C. Lasjaunias, and H. v. Löhneysen, *Solid State Commun.* **49**, 7 (1984).
- <sup>58</sup>M. W. Klein, C. Held, and E. Zuroff, *Phys. Rev. B* **13**, 3576 (1976); M. W. Klein, B. Fischer, A. C. Anderson, and P. J. Anthony, *ibid.* **18**, 5887 (1978).
- <sup>59</sup>D. Moy, R. C. Potter, and A. C. Anderson, *J. Low Temp. Phys.* **52**, 115 (1983).
- <sup>60</sup>G. A. Slack, in *Solid State Physics*, edited by F. Seitz, D. Turnbull, and H. Ehrenreich (Academic, New York, 1979), Vol. 34 p. 1.
- <sup>61</sup>P. P. Peressini, Ph.D. thesis, Cornell University, 1973; Cornell Materials Science Center Report No. 2065 (unpublished).